Proceedings of the 2005 IEEE
International Conference on Robotics and Automation
Barcelona, Spain, April 2005

Dynamics Model of Paramecium Galvanotaxis for Microrobotic Application

Naoko Ogawa*, Hiromasa Oku†‡, Koichi Hashimoto‡† and Masatoshi Ishikawa*

*Graduate School of Information Science and Technology, the University of Tokyo
7–3–1, Hongo, Bunkyo-ku, Tokyo 113–8656, Japan
†PRESTO, Japan Science and Technology Agency
4–1–8 Honcho Kawaguchi-shi, Saitama 332–0012, Japan
‡Graduate School of Information Sciences, Tohoku University
Aramaki Aza Aoba 01, Aoba-ku, Sendai-shi, Miyagi 980–8579, Japan
E-mail: {Naoko_Ogawa,Hiromasa_Oku,Masatoshi_Ishikawa}@ipc.i.u-tokyo.ac.jp, koichi@ic.is.tohoku.ac.jp

Abstract—We propose a dynamics model of galvanotaxis (locomotor response to electrical stimulus) of the protozoan Paramecium. Our purpose is to utilize microorganisms as micro-robots by using galvanotaxis. For precise and advanced actuation, it is necessary to describe the dynamics of galvanotaxis in a mathematical and quantitative manner in the framework of robotics. However, until now the explanation of Paramecium galvanotaxis in previous works has remained only qualitative. In this paper, we construct a novel model of galvanotaxis as a minimal step to utilizing Paramecium cells as micro-robots. Numerical experiments for our model demonstrate realistic behaviors, such as U-turn motions, like those of real cells.

Index Terms—Paramecium, galvanotaxis, dynamics, model, microrobot

I. INTRODUCTION

Today, there is great interest in measurement and control at the micrometer and nanometer scale. Conventional methods, however, have required human operators with high dexterity, expertise, and long experience. Hence, automation technologies to assist operators are needed. Yet, there remain many problems to be solved before its practical application becomes realistic; these problems are mainly due to the still relatively young and undeveloped nature of the field and the limited technology available.

Our approach to overcome these problems is to utilize naturally occurring micromachines, or microorganisms. For all living things, detection of changes in the environment and quick reaction are essential for their survival. There-fore, microorganisms have acquired sophisticated sensors and actuators through the course of their evolution. If we can develop techniques to control them freely, we can realize multi-purpose, programmable microrobotic systems superior to existing micromachine systems. Our goal is to eventually integrate controlled microorganisms and information processing systems [1]. By controlling microorganisms, we aim to achieve various applications, such as cell manipulation, microscopic delivery, smart microsensors, and assembly of micro-electro mechanical systems (MEMS).

To develop microrobotic applications of microorganisms, actuation of cells is a key technology to be realized first. One effective candidate for actuation would be to utilize galvanotaxis, an intrinsic locomotor response to an electrical stimulus, because of its non-invasive and non-contact nature. Using galvanotaxis, some recent studies have achieved simple motion control of *Paramecium caudatum*, a kind of protozoa with strong galvanotaxis [1–3]. However, these studies were based on simple empirical rules without knowledge about the physical properties of the cells, and thus had limited control performance. For instance, when a stimulus was toggled to turn a cell, there was a considerable time lag of several hundred milliseconds between the start of the stimulus and completion of the turn, causing the cell to turn too far [1], [3].

To realize more precise control, it is essential to deal with Paramecium in the framework of standard robotics, that is, to discuss its dynamics, trajectory planning, advanced motion control and so on. The minimal and most basic preparation required for this discussion is a mathematical and quantitative model of the physical dynamics of Paramecium.

Unfortunately, there seem to be no studies on modeling of Paramecium galvanotaxis from such a robotic point of view. Conventional Paramecium models have mainly been physiological and biochemical ones that have focused on its membrane potential or signal transduction, ignoring its physical properties. A very rare physical model proposed by Naitoh *et al.* considered only the behavior with no electrical stimulus [4]. Although Sakane *et al.* and Hirano *et al.* constructed models for chemotaxis and the response called avoiding reaction [5], [6], they are not applicable to galvanotaxis, which has a fundamentally different mechanism from other taxis or reactions. Fearing and Itoh independently performed pioneering experiments on controlling protozoa, but their approach was based on empirical rules [2], [3].

Conventional biology has provided only qualitative explanations for galvanotaxis at the physical level [7], [8]. However, practical application of galvanotaxis requires its quantitative evaluation. Robotic treatment of cells will not become feasible without a mathematical description of single cell motion.

As a minimal preparation for a microrobotic approach to Paramecium control, this paper describes a dynamics model of Paramecium galvanotaxis.

Fig. 1.   Qualitative explanation for galvanotaxis.

Fig. 2.   Schematic representation of forces produced by movements of cilia. Reproduced from reference [4] with modification.
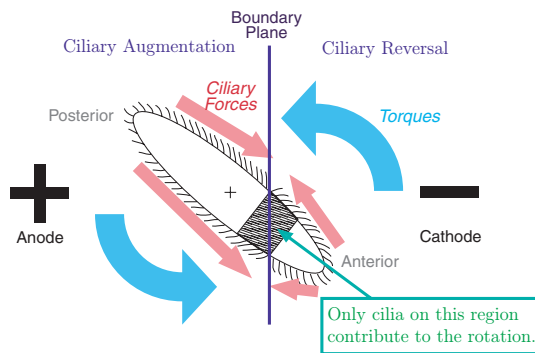
II. MODEL OF GALVANOTAXIS

A. Paramecium and Its Galvanotaxis

1) What is Galvanotaxis?: *Paramecium caudatum* is a kind of unicellular protozoa with an ellipsoidal shape, inhabiting freshwater. It swims by waving cilia on its body; thousands of cilia beat the water backward and yield a forward reaction force [4]. The ciliary motion is controlled by shifts in the membrane potential and the accompanying changes in ion concentration in the cell.

When an external electrical stimulus is applied, it modifies the membrane potential and alters the ciliary movements, consequently exerting an influence on the cell motion. In a macroscopic view, the cell is forced to swim toward the cathode. This phenomenon is called negative galvanotaxis. The term taxis indicates an intrinsic locomotor response toward or away from an external stimulus. Note that galvanotaxis is just a byproduct of the electrophysiological nature of the cell, unlike chemotaxis and phototaxis, which give the cell advantages for its survival.

2) Mechanism of Paramecium Galvanotaxis: A paramecium cell in an electric field shows characteristic ciliary movement. Assume an imaginary plane that is perpendicular to the electric field and located near the center of the cell somewhat close to the cathodal end, dividing the cell into two parts, as illustrated in Fig. 1. By applying the electric field, cilia on the anodal end begin to beat more frequently (ciliary augmentation), and beating on the cathodal end becomes reversed and more frequent (ciliary reversal). This is called the Ludloff phenomenon [9], and it provides a qualitative explanation for galvanotaxis: the asymmetry in direction of the ciliary beatings on the hatched region shown in Fig. 1 generates a rotational force and orients the cell toward the cathode (ciliary motions away from this region are symmetrical and do not contribute to the rotation).

The cause of galvanotaxis can be understood to be a combination of electrochemical, physiological and physical factors. While electrochemical and physiological factors are not so dominant for control performance, physical factors play an important role in control of cells. Therefore, this paper concentrates on physical factors, while regarding electrochemical and physiological ones as black boxes.
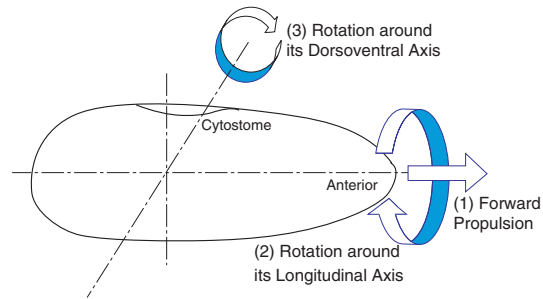
B. Assumptions

1) Simplification of Cell Motion: Strictly speaking, the motion of a Paramecium cell is composed of (1) forward propulsion, (2) a rotation around its longitudinal axis, and (3) a rotation around its dorsoventral axis due to its asymmetrical shape. Consequently, the cell swims forward spinning along a spiral [4]. The most dominant element in galvanotaxis is element (1). For simplicity, we will not discuss the other two elements, which are not essential for galvanotaxis. This assumption means that the cell just goes straight when there is no electric field.

By disregarding the rotation components, we can describe the cell motion in a two-dimensional plane including the cell axis and the electric field vector. Hereafter we consider cell motion only in this plane. At the same time, because motions of the cilia can be assumed to be symmetric with respect to the plane, the movements of the cilia on the plane can sufficiently represent the movements of all cilia. Thus, we consider the cell as a two-dimensional ellipsoid on the plane.

2) Assumptions on Ciliary Motion: We assume that cilia are distributed uniformly on the edge of the ellipsoid with linear density n. For simplicity, we consider only two states for beating, reverse and normal. The cilia are oriented towards the anterior side in reverse beating, and towards the posterior side in normal beating. In the presence of an electric field, imagine a plane perpendicular to the field (hereinafter referred to as "a boundary plane"). This plane divides the cell into two regions; cilia are considered to be normal in the anodal side, and reversed in the cathodal side. The boundary plane is formed in the cathodal side, and the shortest distance between the plane and the center of the cell is l.

The beating frequency is assumed to be uniform over the whole cell, with a value φ_0 in the absence of an electric field (hereinafter referred to as "regular state"). When an electric field E is applied, the frequency increases to $\varphi = (1 + \beta E)\varphi_0$ ($\beta > 0$). Let f_0 be a propulsion force yielded by one cilium in the regular state, the force being proportional to the frequency φ_0 ($f_0 = \alpha\varphi_0$). Let $f = \alpha\varphi = (1 + \beta E)f_0$ be the force in the presence of the electric field.

3) Coordinate Systems: We define two coordinate systems, a global one (X, Y) and a local one (x, y), on the plane, as shown in Fig. 3. The global coordinate system is allocentric,
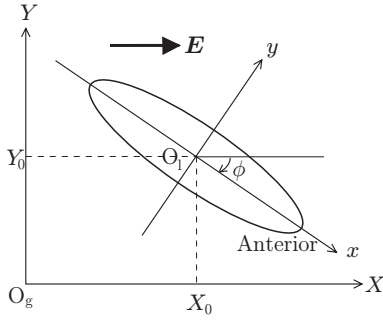
Fig. 3. Relation between the global coordinate system (X, Y) and the local coordinate system (x, y).
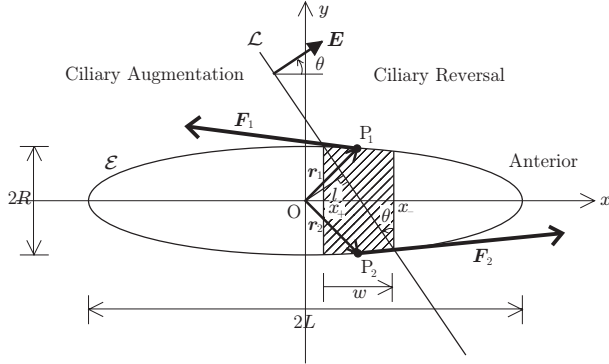
Fig. 4. Parameters in the local coordinate system.

that is, fixed with respect to the external world, with the X-axis parallel to E. The local coordinate system (introduced to simplify the description) is egocentric, that is, fixed with respect to the cell, with the X-axis parallel to the longitudinal axis of the cell. Let ϕ be the angle of the cell axis in the global coordinate system ($\phi < 0$ in Fig. 3, for the sake of convenience in deriving the model).

Let the cell shape be an ellipsoid with a major axis $2L$ and a minor axis $2R$ ($L > R$). In the local coordinate system, the cell is represented as an ellipsoid $\mathcal{E}$:

$$\mathcal{E}: \frac{x^2}{L^2} + \frac{y^2}{R^2} = 1. \tag{1}$$

C. Model of the Torque

The phenomenon whereby a Paramecium cell swims toward the cathode is due to a torque caused by assymmetry of ciliary motion. In this section, we estimate this torque. First, consider an ellipsoid $\mathcal{E}$, as illustrated in Fig. 4.

For convenience, let us introduce $\theta = -\phi$, as the angle of the electric field in the local coordinate system. Then the boundary plane is expressed as a line $\mathcal{L}$:

$$\mathcal{L}: y = -\frac{1}{\tan\theta}x + \frac{l}{\sin\theta}. \tag{2}$$

As mentioned in the former section, assymmetry of ciliary beating exists only at the substantially trapezoidal region formed by the intersection of the boundary plane and the ellipsoid (shown as hatched regions in Fig. 1 and Fig. 4). The

forces excerted by cilia outside this region are symmetrical and do not contribute to rotation. Thus, we consider only the forces generated at this trapezoidal region.

The x positions of two lines that consist of the "upper" side and "lower" side of the trapezoid are equal to those of two intersecting points of $\mathcal{E}$ and $\mathcal{L}$. These two positions, x_- and x_+, are obtained as two roots of equation

$$(R^2 \sin^2\theta + L^2 \cos^2\theta)x^2 - 2lL^2\cos\theta \cdot x$$
$$+ l^2 L^2 - R^2 L^2 \sin^2\theta = 0, \tag{3}$$

which is derived by eliminating y from Eq. (1) and Eq. (2) (this equation always has two real roots). Between these two intersecting points of $\mathcal{E}$ and $\mathcal{L}$, let x_+ be a point with larger y position, and x_- be a point with smaller y position.

Because it would be too complicated to consider all minuscule forces generated by each cilium, here we focus on the resultant forces for simplicity. We set the sites of action, $P_1(x_a, y_a)$ and $P_2(x_a, -y_a)$ ($y_a \geq 0$), on the midpoints of the "height" of the trapezoid, and assume the directions of the forces to be tangential to the ellipsoid. Let us define the disposition vectors, $r_1 = \overrightarrow{OP_1}$ and $r_2 = \overrightarrow{OP_2}$.

Then we obtain

$$x_a = \frac{x_- + x_+}{2} = \frac{lL^2\cos\theta}{R^2\sin^2\theta + L^2\cos^2\theta}. \tag{4}$$

Also, y_a is obtained by substituting Eq. (4) into Eq. (1):

$$y_a = \frac{R}{L}\sqrt{L^2 - x_a^2}.$$

The two tangential lines on the sites of action $(x_a, \pm y_a)$ are given by

$$\frac{x_a}{L^2}x \pm \frac{y_a}{R^2}y = 1,$$

from which we get the inclinations of the two tangential lines,

$$m = \mp\frac{R^2 x_a}{L^2 y_a},$$

and we get normalized tangent vectors

$$\left(\frac{1}{\sqrt{1+m^2}}, \frac{m}{\sqrt{1+m^2}}\right).$$

Let m_1 be the tangent vector at P_1, and m_2 be that at P_2. Then unit force vectors, e_1 at P_1 and e_2 at P_2, are:

$$e_1 = -m_1 \quad \text{(reverse beating)},$$
$$e_2 = m_2 \quad \text{(normal beating)},$$

considering the directions of ciliary beatings.

Moreover, let us suppose that the magnitude of the resultant force is proportional to the number of cilia n, and that n is proportional to the "height" of the trapezoid:

$$w = x_- - x_+,$$

which is a signed value whose sign is the same as θ. Then the propelling forces F_1 and F_2 at the points P_1 and P_2 respectively, are written as

$$F_1 = fwne_1, \quad F_2 = fwne_2.$$

By assuming that the center of gravity of the cell is located at the center of the ellipsoid, we find the torques at the points P_1 and P_2:

$$\boldsymbol{\tau}_1 = \boldsymbol{r}_1 \times \boldsymbol{F}_1, \quad \boldsymbol{\tau}_2 = \boldsymbol{r}_2 \times \boldsymbol{F}_2,$$

where one should note that these vectors are treated as three dimensional in calculating cross products.

Finally the torque rotating the cell body is given by:

$$\boldsymbol{\tau} = \boldsymbol{\tau}_1 + \boldsymbol{\tau}_2.$$

Since its x and y components are obviously zero, hereafter we call its z component, τ_z, the "torque".

Finally, by substituting $\phi = -\theta$, the torque is described in the global coordinate system as:

$$\tau_z(\phi)$$
$$= -\frac{4LR^2 fns\sqrt{L^2c^2 + R^2s^2 - l^2}}{\sqrt{L^4c^4 + 2L^2R^2c^2s^2 + R^4s^4 - L^2l^2c^2 + R^2l^2c^2}}, \quad (5)$$

where $\quad s = \sin\phi, c = \cos\phi$.

This equation provides the torque generated in the Paramecium cell with the angle ϕ.

D. Dynamic Equation of Paramecium Cell

Using the torque estimated in previous section, we now discuss the motion equation of a Paramecium cell.

1) Dynamic Equation for Translational Motion: In the micrometer-scale world the Paramecium cells inhabit, the inertial resistance of the fluid is small enough to be negligible, and the viscous resistance becomes dominant instead. Hence we can apply Stokes' law, derived from the Navier-Stokes equation by ignoring inertial force.

Since the rigorous evaluation of viscous resistance around an ellipsoid is quite complicated, here we approximate the viscosity roughly by applying the formula for a sphere as a substitute. According to Stokes' law, the force exerted on a sphere with radius a, moving with velocity v in a viscous fluid is given by

$$F_s = 6\pi\mu a v, \quad (6)$$

where μ is the viscosity of the fluid. From this equation, the viscous force around the ellipsoidal cell can be obtained by replacing the radius a by the cell radius R. Thus the motion equation for the translational motion of the cell can be roughly approximated by:

$$M\ddot{\boldsymbol{X}} + D\dot{\boldsymbol{X}} = \boldsymbol{F}, \quad (7)$$

where $\boldsymbol{X} = (X, Y)^t$ is the cell position, $\boldsymbol{F} = 2fn|x_a|\boldsymbol{e_X}$ is a forward propulsive force, $\boldsymbol{e_X} = \frac{\boldsymbol{X}}{|\boldsymbol{X}|} = (\cos\phi, \sin\phi)^t$ is a unit vector along the body axis, $D = 6\pi\mu R$ is the viscous friction coefficient, $M = \rho V$ is the cell mass, ρ is the cell density, and $V = 4\pi LR^2/3$ is the cell volume.

2) Dynamic Equation for Rotational Motion: We now derive a motion equation for rotational motion. As mentioned above, because evaluation of the viscosity around the ellipsoid is complicated, we again substitute Stokes' law for a sphere. A viscous resistance torque against the rotation can be approximated by assuming two mass points on the body axis at a quarter of the length $(L/2)$ from the origin, substituting $v = \dot{\phi} \cdot L/2$ and $a = L/2$ into the Stokes' law equation (6), and multiplying both sides by $L/2$:

$$\tau_s = F_s\frac{L}{2} = 6\pi\mu\frac{L}{2}\dot{\phi}\frac{L}{2}\frac{L}{2} = \frac{3}{2}\pi\mu L^3\dot{\phi}.$$

This derivation would be too rough and the coefficient $3/2$ might be unreliable; there could be a model error of several fold. Let us introduce δ to replace the coefficient and absorb the error. Thus, the motion equation for rotational motion is given by

$$I\ddot{\phi} + D'\dot{\phi} = \tau(\phi), \quad (8)$$

where $I = \pi M(R^2 + L^2)/5$ is the moment of inertia for an ellipsoid, and $D' = \delta\pi\mu L^3$ is the viscous friction coefficient.

3) Integration of Motion Equations: Integration of the motion equations for translational motion (7) and rotational motion (8) leads to the following equations:

$$\dot{\boldsymbol{y}} = A\boldsymbol{y} + \boldsymbol{B}(\boldsymbol{y}), \quad (9)$$

$$A = \begin{pmatrix} 0 & 0 & 1 & 0 & 0 & 0 \\ 0 & 0 & 0 & 1 & 0 & 0 \\ 0 & 0 & -D/M & 0 & 0 & 0 \\ 0 & 0 & 0 & -D/M & 0 & 0 \\ 0 & 0 & 0 & 0 & 0 & 1 \\ 0 & 0 & 0 & 0 & 0 & -D'/I \end{pmatrix},$$

$$\boldsymbol{B}(\boldsymbol{y}) = \left(0, 0, \frac{P}{M}\cos\phi, \frac{P}{M}\sin\phi, 0, \frac{\tau_z(\phi)}{I}\right)^t,$$

and where $P = 2fn|x_a|$ and $\boldsymbol{y} = (X, Y, \dot{X}, \dot{Y}, \phi, \dot{\phi})^t$.

III. NUMERICAL EXPERIMENTS AND COMPARISON TO ACTUAL DATA

We performed some numerical experiments to verify the motion equation (9) by using numerical analysis software (MATLAB, MathWorks Inc.).

A. Preparation of Parameters

Table I shows several physical parameters used in the experiments. We obtained the cell size by observing cells incubated in our laboratory; the size we observed was smaller than the average [8]. The boundary plane offset l is estimated from several figures shown in previous studies [8], [10], for it is difficult to observe with our equipment. As for β, the increase in beating frequency with electric field, the value was estimated from the fact that the frequency almost doubled to around 50 Hz under a stimulation of around a few volts per centimeter, while that in the regular state was around 15-20 Hz [4].

TABLE I

PARAMETERS OF THE PROPOSED MODEL.

Parameters	Values	Comments
Major cell axis $2L$	$100\,\mu$m	our strain
Minor cell axis $2R$	$25\,\mu$m	our strain
Boundary plane offset l	$10\,\mu$m	Reference [8], [10]
Viscosity of water μ	1.00×10^{-3} kg/(ms)	at 20 ℃
Cell density ρ	$1,000$ kg/m^3	same as water
Increase in beating freq. β	2.00×10^{-3} V^{-1}	
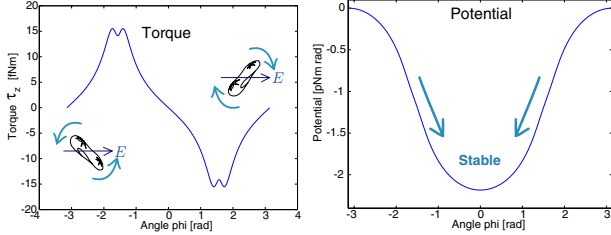
Fig. 5. Torque $\tau_z(\phi)$ generated by ciliary force (left) and its potential energy (right).

The force yielded by cilia on unit length, $f_0 n$, is still an unknown parameter. We estimated the order of $f_0 n$ by using the actual value of swimming velocity measured in past experiments.

The terminal velocity of a cell in the regular state was obtained by substituting $\ddot{\boldsymbol{X}} = \boldsymbol{0}$ into eq. (7) under conditions $E = 0$ and $\phi = 0$:

$$\dot{\boldsymbol{X}} = \boldsymbol{F}/D = \frac{|x_a|_{\phi=0}\boldsymbol{e_X}}{3\pi\mu R} f_0 n.$$

Since x_a equals to l at $E = 0$, we can estimate $f_0 n$ by:

$$f_0 n = \frac{3\pi\mu R}{l} |\dot{\boldsymbol{X}}|. \tag{10}$$

According to our measurement of the cell velocity by using a high-speed vision system [11], their velocity is around 400μm/s. Using this, we estimated $f_0 n$ to be 4.71×10^{-6} N/m.

B. Torque Profile $\tau_z(\phi)$

The left side of Fig. 5 shows the torque $\tau_z(\phi)$ as a function of ϕ. The torque affects the cell so as to decrease ϕ, that is, to make the cell turn toward the cathode.

C. Angular Stability in the Proposed Model

Equations (7) and (8) indicate that the motion equation of a Paramecium cell has nonlinearity that might make the model unstable. However, when the angle ϕ is sufficiently small, that is, the direction of the cell is close to that of the electric field, it is possible to make the model linear approximately. In this section, we will linearize the model to observe the stability for small ϕ.

In Fig. 5, the z component of the torque, $\tau_z(\phi)$, exhibits a gradual monotonic decrease near $\phi = 0$, which implies that it can be regarded as linear with respect to ϕ in this area.

Therefore, $\tau_z(\phi)$ can be approximated using the inclination of the tangential line at $\phi = 0$:

$$\tau_z(\phi) \simeq \left.\frac{\mathrm{d}\tau_z}{\mathrm{d}\phi}\right|_{\phi=0} \cdot \phi = -4\frac{R^2 L f n \sqrt{L^2 - l^2}}{\sqrt{L^4 - L^2 l^2 + R^2 l^2}}\phi.$$

Then eq. (8) becomes:

$$\ddot{\phi} = -\frac{D'}{I}\dot{\phi} + \frac{Q}{I}\phi, \quad \text{where} \quad Q = -4\frac{R^2 L f n \sqrt{L^2 - l^2}}{\sqrt{L^4 - L^2 l^2 + R^2 l^2}}.$$

By defining a state variable $\tilde{\boldsymbol{y}} = (\phi, \dot{\phi})^{\mathrm{t}}$, the model of the cell rotation becomes linear around the origin:

$$\dot{\tilde{\boldsymbol{y}}} = \tilde{A}\tilde{\boldsymbol{y}}, \quad \tilde{A} = \begin{pmatrix} 0 & 1 \\ Q/I & -D'/I \end{pmatrix}.$$

The eigenvalues of this matrix $\tilde{A}$ are $\left(-D' \pm \sqrt{D'^2 - 4IQ}\right)/2I$, which are negative. Therefore, the cell is stable for small ϕ and its direction converges to $\phi = 0$.

In addition, the global stability was verified qualitatively by calculating a potential energy U for rotation. We defined U as $\tau_z = -\frac{\partial U}{\partial \phi}$ and computed it by numerical integration of eq. (5) with respect to ϕ. The right side of Fig. 5 shows the profile of U, indicating that the cell tends to approach $\phi = 0$ for all ϕ.

D. Simulation and Comparison of U-turn Motions

We have accumulated a large amount of data for Paramecium motion using a high-speed vision system called I-CPV (Fig. 6 A) [12] and a galvanotaxis continuous observation system (Fig. 6 B) [13]. Using these data, we adjusted the parameter δ to be 7.5, and verified the validity of the model.

When an electric field is applied in the direction opposite to the swimming direction of a cell, the cell makes a U-turn motion (Fig. 6 C). We tested whether our proposed model can demonstrate this phenomenon.

First, swimming trajectories for cells with eleven different initial orientations were calculated. Figure 6 D demonstrates all trajectories simultaneously. The cells were configured to all have the same initial position, namely, on the origin $(0, 0)$, but not their initial angles, which differed by intervals of $30°(-150°, -120°, \ldots, 150°)$. A 5.0-V/cm electric field was applied along the X-axis. The trajectory of each cell was calculated using an ordinary differential equation solver. As shown in Fig. 6 D, all cells starting from the origin turned toward the cathode, like the real ones.

Next, we compared simulated and experimental positions as shown in Fig. 7. We extracted positions along the electric field (X direction), because X-position is almost independent of fluctuations caused by spiral motions, which we disregarded.

Experimental data (thin lines) were obtained by high-speed measurement of the responses of a single cell for several levels of input electric field, using the galvanotaxis continuous measurement system [13]. The electric field applied to the cell had a step-like form, rising to 4.1 V/cm, and its position and angle were continuously measured at a 1-kHz frame rate
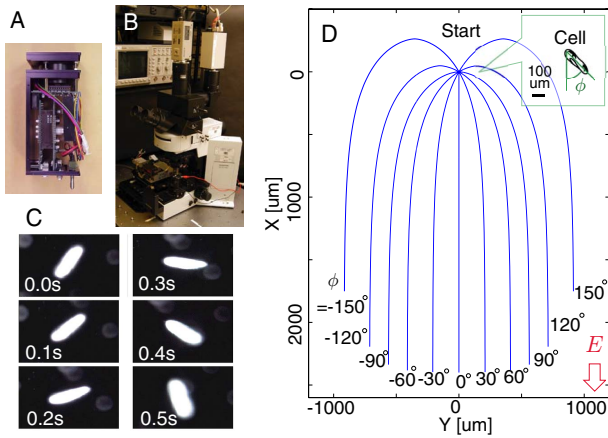
Fig. 6. A: High-speed vision system (I-CPV) [12]. B: Galvanotaxis continuous observation system [13]. C: U-turn motion observed by our system [13]. D: Demonstration of U-turn motions of cells.
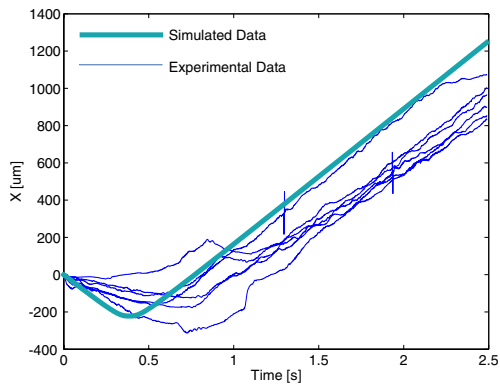
Fig. 7. Comparison between simulated data (thick line) and experimental data (thin lines).

by high-speed tracking using the I-CPV system [11], [12]. In Fig. 7, data for three seconds from the stimulus change in six trials are overlaid. Simulated data (thick line) was calculated under the conditions that the initial angle was the average of angles obtained from previously measured data. The simulated data was approximately in agreement with the experimental results.

E. Responses for Various Inputs

We investigated how the cell response is influenced by the changes in the control inputs (the magnitude and direction of the electric field). This time, we focused on the time needed for the U-turn motion (U-turn time), defined as the time from the initial position to the moment it reached $\phi = 15°$. The default values for the magnitude of the electric field and the initial angle were set to 5 V/cm and 165 °, respectively.

The left plot in Fig. 8 shows the relation between the magnitude of electric field and the U-turn time, and the right plot shows that between the angle of electric field and the U-turn time. As predicted, the U-turn time decreases as the magnitude increases or the angle decreases.
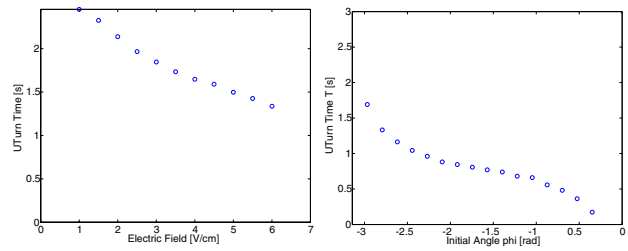
Fig. 8. Relationship between the electric field E and the U-turn time (left), and between the voltage angle ϕ and the U-turn time (right).

F. Toward the Application of Cell Control

Unlike robots, living things do not always exhibit uniform behavior under the same conditions, and there exists quite large differences among individuals. These facts would make it quite difficult to realize model-based control using the proposed model directly. Nevertheless, we believe that even the estimation of U-turn time or trajectories allows more precise and advanced control.

IV. SUMMARY

In this paper, we proposed a physical model of Paramecium galvanotaxis as the first step for microrobotic application of microorganisms, and investigated its behavior by numerical calculations and experiments.

REFERENCES

[1] N. Ogawa, H. Oku, K. Hashimoto, and M. Ishikawa, "Motile cell galvanotaxis control using high-speed tracking system," in *Proc. 2004 IEEE Int. Conf. Robotics and Automation (ICRA 2004)*, Apr. 2004, pp. 1646–1651.
[2] R. S. Fearing, "Control of a micro-organism as a prototype micro-robot," in *2nd Int. Symp. Micromachines and Human Sciences*, Oct. 1991.
[3] A. Itoh, "Motion control of protozoa for bio MEMS," *IEEE/ASME Trans. Mechatronics*, vol. 5, no. 2, pp. 181–188, June 2000.
[4] Y. Naitoh and K. Sugino, "Ciliary movement and its control in *Paramecium*," *J. Protozool.*, vol. 31, no. 1, pp. 31–40, 1984.
[5] A. Sakane, K. Hashigami, T. Tsuji, H. Ohtake, and M. Kaneko, "Model of taxis of paramecia based on the Hodgkin-Huxley equations," in *Proc. 2001 JSME Conference on Robotics and Mechatronics (Robomec'01)*, Jul. 2001 (in Japanese), pp. 2P2–B9.
[6] A. Hirano, M. Suzuki, T. Tsuji, N. Takiguchi, and H. Ohtake, "Mobile robot control based on chemotaxis of paramecia," in *Proc. 2004 JSME Conference on Robotics and Mechatronics (Robomec'04)*, Jun. 2004 (in Japanese), pp. 1A1–L1–23.
[7] H.-D. Görtz, Ed., *Paramecium*. Springer-Verlag, 1988.
[8] H. S. Jennings, *Behavior of the Lower Organisms*. Columbia University Press, 1923.
[9] K. Ludloff, "Untersuchungen über den Galvanotropismus," *Archiv fur die Gesamte Physiologie*, vol. 59, pp. 525–554, 1895.
[10] T. Kamada, "Polar effect of electric current on the ciliary movements of Paramecium," *Journal of the Faculty of Science, Imperial University of Tokyo, Sect. IV, Zoology*, vol. 2, pp. 285–298, 1931.
[11] H. Oku, N. Ogawa, K. Hashimoto, and M. Ishikawa, "Two- dimensional tracking of a motile microorganism allowing high-resolution observation with various imaging techniques," *Rev. Scientific Instruments*, vol. 76, no. 3, Mar. 2005 (to appear).
[12] H. Toyoda, N. Mukohzaka, K. Nakamura, M. Takumi, S. Mizuno, and M. Ishikawa, "1ms column-parallel vision system coupled with an image intensifier; I-CPV," in *Proc. Symp. High Speed Photography and Photonics 2001*, vol. 5-1, 2001, pp. 89–92, (in Japanese).
[13] N. Ogawa, H. Oku, K. Hashimoto, and M. Ishikawa, "Single-cell level continuous observation of microorganism galvanotaxis using high-speed vision," in *Proc. 2004 IEEE Int. Symp. Biomedical Imaging (ISBI 2004)*, Apr. 2004, pp. 1331–1334.